ELSEVIER

Journal of Alloys and Compounds 239 (1996) 63–70

Journal of ALLOYS AND COMPOUNDS

The Ti-based metal hydride electrode for Ni–MH rechargeable batteries

Han-Ho Lee, Ki-Young Lee, Jai-Young Lee*

Department of Materials Science and Engineering, Korea Advanced Institute of Science and Technology, Kusong-dong 373-1, Yusung-gu, Taejon 305-701, South Korea

Received 3 January 1996

Abstract

The pressure–composition isotherms and electrochemical characteristics of titanium-based hydrogen storage alloys have been studied for various compositions. In the Ti–Zr–V–Mn–Ni system, $Ti_{0.2}Zr_{0.05}V_{0.4}Mn_{0.35-x}Ni_x$ ($x = 0.1$–0.25) alloys were found to have a large hydrogen storage capacity (greater than 1.75 wt.% g^{-1} alloy) and high discharge capacity (350–440 mA h g^{-1}). Their structure was confirmed to be multi-phase and composed of an AB_2-type C14 Laves phase matrix and V-rich b.c.c. second phase by using X-ray diffraction, scanning electron microscope and electron microprobe analyses. In order to identify the contribution of each phase to the high discharge capacity of multi-phase alloys, these two phases were prepared separately and their hydrogen storage capacities were investigated. It was found that the V-rich b.c.c. second phase was hardly hydrogenated in KOH electrolyte, though its theoretical hydrogen storage capacity was as high as 1.93 wt.% H g^{-1} alloy as determined from the pressure–composition isotherms in the solid–gas reaction. Its potential hydrogen storage capacity was able to be utilized by the presence of a C14 matrix phase which had a catalytic activity for the charge-transfer reaction in KOH electrolyte.

Keywords: Metal hydride electrode; Discharge capacity; Hydrogen sorption; Hydrogen storage; Pressure–composition isotherms

1. Introduction

The nickel–metal hydride (Ni–MH) battery has several advantages, such as high energy density, more tolerance to overcharge and overdischarge, high-rate capability and non-toxic materials in comparison with the conventional lead–acid and/or nickel–cadmium batteries [1–3]. The small size Ni–MH batteries (AA size) have been commercialized for portable electronic appliances while the large size Ni–MH batteries are under development for electric vehicles. The Ni–MH batteries for electric vehicles require higher energy density and power density. It is especially required to increase the energy density above 60–70 W h kg^{-1}, which is the energy density of the commercialized Ni–MH batteries [4,5]. The energy density of the Ni–MH battery depends on the discharge capacities of both the electrodes (NiOOH and MH) and the construction of the cell. However, it is difficult to increase the discharge capacity of the nickel electrode significantly because its charge–discharge efficiency has been improved as high as 90% and its theoretical discharge capacity is limited to 290 mA h g^{-1} [6,7]. In contrast to the positive nickel electrode, there remains more room for improvement of the discharge capacity of the negative MH electrode because the hydrogen storage capacity of the metal hydride can be increased by developing light high-capacity alloys.

Two major requirements should be satisfied to develop a high capacity MH electrode material. Firstly, in order to improve the theoretical capacity, the reversible hydrogen storage capacity of the metal hydride should be high in the solid–gas reaction, maintaining the desorption pressure in the range of 0.01–1 atm at room temperature [8]. Secondly, in order to utilize the theoretical capacity efficiently, the metal hydride should have a high catalytic activity on the charge transfer reaction for the electrochemical hydrogenation in KOH electrolyte. The electrochemical hydrogenation is composed of three consecutive steps which are the hydrogen diffusion in the MH bulk, the hydrogen transfer between absorbed and

* Corresponding author.

PII S0925-8388(96)02276-1

adsorbed states and the electrochemical oxidation/reduction of hydrogen at the interface between the alloy surface and the electrolyte [9]. The last step is known to be a charge transfer reaction and it can be improved by a catalyst, such as nickel, contained in the MH as an alloying element.

So far, several metal hydride systems have been developed as negative electrode materials and major consideration has been given to Ti–Ni [10,11], Zr–V–Ni [12,13], $ZrMn_2$ [14], Zr–Cr–Ni [15] and $MmNi_5$ [16–18] systems. However, the electrochemical discharge capacities of those alloy systems are less than 400 mA h g^{-1} because reversible hydrogen storage capacities are lower than 1.5 wt.% H g^{-1} alloy at room temperature in the gas–solid reaction, as verified by the *P–C* isotherms (*P–C* isotherms). Recently, titanium-based alloy systems such as $TiCr_2$ and $TiMn_2$ have been of great interest as promising candidates for the high capacity electrode materials. The structures of those AB_2-type alloys are C15 or C14 Laves phases. In the alloy development of both systems, it is very important to keep the Laves phase structure. The $TiMn_2$-based intermetallic compounds have a wider compositional range of phase homogeneity than $TiCr_2$-based intermetallic compounds, and its gas–solid hydrogenation characteristics deteriorate less on substitution of alloying elements. So, many researchers were devoted to development of $TiMn_2$-based compounds for hydrogen storage alloys [19–21]. However, $TiMn_2$-based compounds have not been investigated for the electrode materials so far, because those researches have been focused on improving gaseous hydrogenation characteristics for the application of hydrogen storage systems which require equilibrium hydrogen desorption pressures of 5–10 atm at room temperature.

In this study, $TiMn_2$-based C14-type Laves phase intermetallic compound was modified by substituting alloying elements such as Zr, V and Ni in order to develop a high capacity MH electrode material, and its gaseous and electrochemical hydrogenation characteristics were investigated.

2. Experimental details

The Ti–Mn-based hydrogen storage alloys used in this study were prepared by arc-melting in an argon atmosphere and were remelted several times in order to ensure homogeneity. These alloys were crushed and mechanically ground into powders in air and sieved to − 325 mesh. To investigate the gaseous hydrogenation characteristics in the gas–solid reaction, the *P–C* isotherms for hydrogen desorption were measured by an automatic Sieverts-type apparatus. Also, in order to identify the crystal structure and the phases of the hydrogen storage alloy, X-ray diffraction (XRD) measurements and scanning electron microscope (SEM) analysis were performed respectively.

To prepare MH negative electrodes, 0.2–0.3 g of alloy powders were mixed with 10 wt.% of nickel powders as a current collector and 10 wt.% of polytetrafluoroethylene (PTFE) powders as a binder, and then pressed at 5 ton cm^{-2} into a pellet of 10 mm diameter and about 1 mm thickness. A half-cell was constructed using a platinum wire as a counter electrode and mercury/mercury oxide (Hg/HgO) as a reference electrode in 30 wt.% KOH electrolyte. The electrodes were charged for 10 h and discharged to − 0.7 V (vs. Hg/HgO) at a current density of 50 mA g^{-1}.

3. Results and discussion

3.1. The gaseous hydrogenation characteristics of the Ti–Mn–M (M = Al, Cu, Cr, Fe, Ni, V) system

In the Ti–Mn binary system, there are various phases such as β-Ti solid solution of b.c.c. structure, α-Ti solid solution of hexagonal structure, $TiMn_2$ intermetallic compound of $MgZn_2$-type hexagonal C14 Laves phase, $TiMn_3$, $TiMn_4$ intermetallic compounds and α-, β-, γ-, δ-Mn solid solutions [22]. Among these phases, solid solution-type phases are not suitable for the starting system in the development of MH electrode materials because α and β-Ti solid solutions form too stable a hydride, and Mn-based solid solutions do not absorb hydrogen. In contrast, $TiMn_2$ Laves phase is a favorable starting system for the MH electrode material because its gaseous hydrogenation reaction is very fast and its reversible hydrogen storage capacity is high [19]. However, its equilibrium desorption pressure should be decreased because the equilibrium pressure is as high as 30 atm [23]. The equilibrium pressure can be decreased to 7 atm at room temperature by increasing the titanium content to $Ti_{0.4}Mn_{0.6}$. However, the equilibrium pressure should be decreased below 1 atm by substituting alloying elements. The effects of the alloying elements were investigated by measuring *P–C* isotherms of $Ti_{0.4}Mn_{0.4}X_{0.2}$ (X = Al, Cr, Cu, Ni, Fe) alloys at 30°C as shown in Fig. 1. Although hydrogen absorption capacity increased considerably, the reversible hydrogen capacity decreased greatly, especially for the *P–C* isotherms of $Ti_{0.4}Mn_{0.4}X_{0.2}$ (*X = Al*, Cu, Ni) alloys. The reversible capacities of $Ti_{0.4}Mn_{0.4}Cr_{0.2}$ and $Ti_{0.4}Mn_{0.4}Fe_{0.2}$ were only 0.5 H/M when maintaining almost the same equilibrium pressure. The XRD patterns of these alloys are shown in Fig. 2. It was found that the crystal structure of $Ti_{0.4}Mn_{0.6}$ was mainly C14 Laves phase and those of $Ti_{0.4}Mn_{0.4}X_{0.2}$

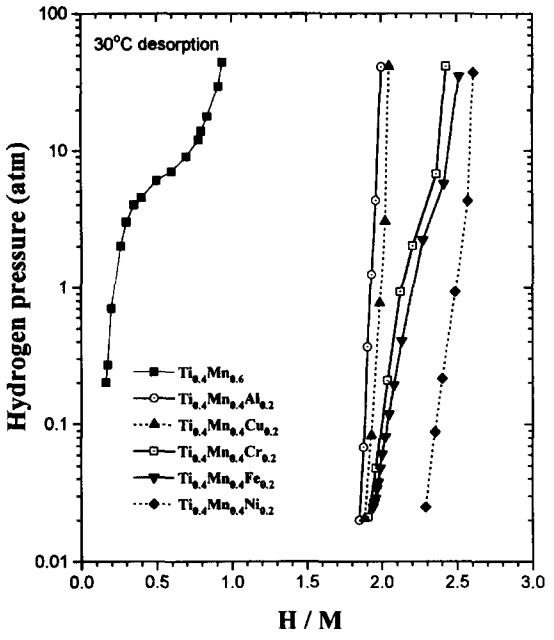

Fig. 1. Desorption P–C isotherms of $Ti_{0.4}Mn_{0.4}X_{0.2}$ (X = Mn, Al, Cu, Cr, Fe, Ni) alloys at 30°C.

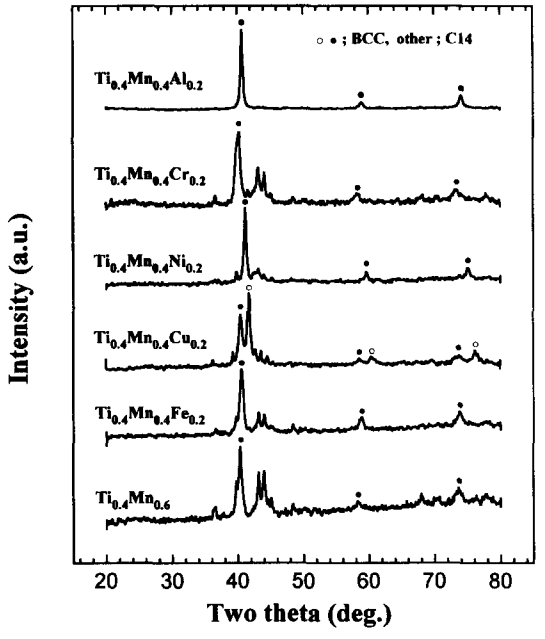

Fig. 2. XRD patterns of $Ti_{0.4}Mn_{0.4}X_{0.2}$ (X = Mn, Al, Cu, Cr, Fe, Ni) alloys.

(X = Al, Cu, Ni) alloys were mainly b.c.c., whilst those of $Ti_{0.4}Mn_{0.4}Cr_{0.2}$ and $Ti_{0.4}Mn_{0.4}Fe_{0.2}$ alloys were b.c.c. containing some C14 Laves phase. It was found that the reversible hydrogen storage capacity was correlated with the existence of the C14 Laves phase; however, the reversible hydrogen storage capacity was not improved by substituting Al, Cu, Cr, Fe or Ni for Mn because the β-Ti phase of the $Ti_{0.4}Mn_{0.6}$ alloy was stabilized by the substitution of transition elements.

When vanadium was substituted in $Ti_{0.4}Mn_{0.6}$ alloy, the crystal structure was maintained as a C14 Laves phase at a certain composition and the equilibrium pressure decreased below 1 atm without decreasing the hydrogen storage capacity considerably. Desorption P–C isotherms and XRD patterns of Ti–V–Mn alloys are shown in Figs. 3 and 4 respectively. It was found that $Ti_{0.4}V_{0.3}Mn_{0.3}$ and $Ti_{0.3}V_{0.4}Mn_{0.3}$ alloys, which were mainly composed of a Ti-based b.c.c. structure, had less reversible hydrogen capacity than

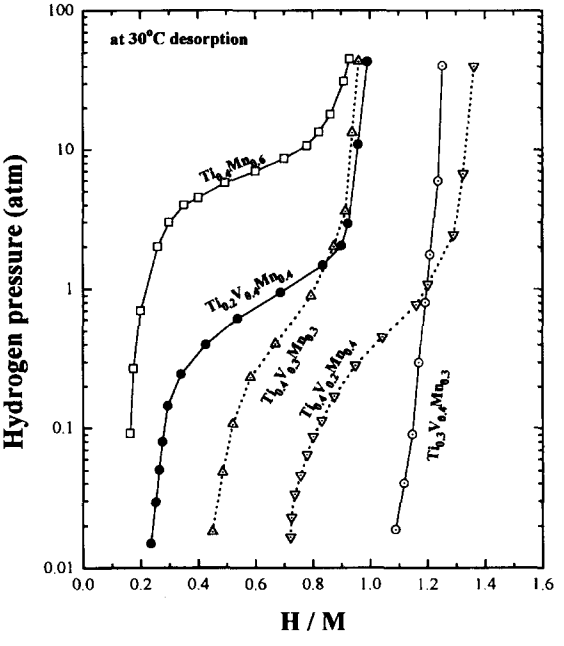

Fig. 3. Desorption P–C isotherms of Ti–V–Mn alloys at 30°C.

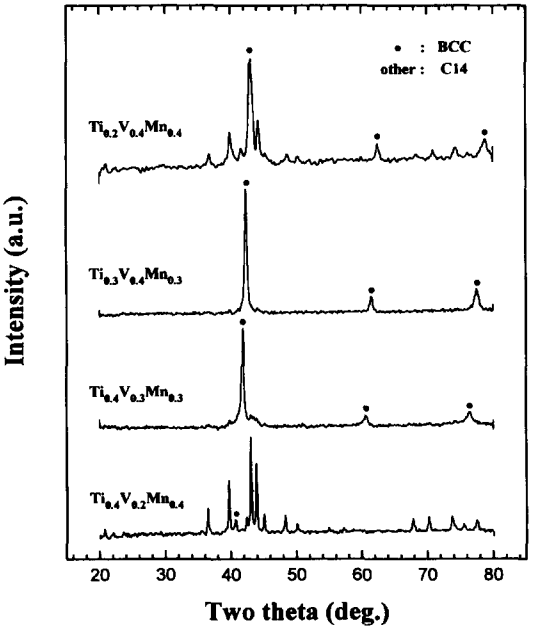

Fig. 4. XRD patterns of Ti–V–Mn alloys.

$Ti_{0.2}V_{0.4}Mn_{0.4}$ and $Ti_{0.4}V_{0.2}Mn_{0.4}$ alloys, which were mainly composed of C14 Laves structure. So, it seems that $Ti_{0.2}V_{0.4}Mn_{0.4}$ and $Ti_{0.4}V_{0.2}Mn_{0.4}$ alloys have suitable gaseous hydrogenation characteristics for the negative electrode material because the equilibrium desorption pressure is between 0.01 and 1 atm and the reversible hydrogen storage capacity is above 1.44 wt.% H g^{-1} alloy.

3.2. The electrochemical characteristics of the Ti–V–Mn–Ni system

Although $Ti_{0.4}V_{0.2}Mn_{0.4}$ and $Ti_{0.4}V_{0.2}Mn_{0.4}$ alloys had good hydrogenation properties in the solid–gas reaction, these alloys could not electrochemically absorb hydrogen in KOH electrolyte. Fig. 5 shows charging–discharging curves of $Ti_{0.4}V_{0.2}Mn_{0.4}$ alloy after several cycles and $Ti_{0.4}V_{0.2}Mn_{0.2}Ni_{0.2}$ alloy after the first cycle. In the case of $Ti_{0.4}V_{0.2}Mn_{0.4}$ alloy, the electrode potential exceeded − 0.932 V (vs. Hg/HgO) of the hydrogen evolution potential during the charging period, and dropped drastically below − 0.7 V as soon as the electrode was discharged, as shown in Fig. 5. During the charging period of the $Ti_{0.4}V_{0.2}Mn_{0.4}$ alloy, only the hydrogen gas evolution reaction proceeded instead of the electrochemical hydrogen absorption reaction. It was supposed that this behavior was due to the existence of passive films and the lack of an electrochemical catalytic phase on the surface. In this work, for the $Ti_{0.4}V_{0.2}Mn_{0.4}$ alloys, manganese was partially substituted by nickel, which had a catalytic activity for electrochemical hydrogenation. In charging–discharging curves of $Ti_{0.4}V_{0.2}Mn_{0.2}Ni_{0.2}$ alloy after the first cycle, as shown in Fig. 5, the electrode potential decreased below the hydrogen evolution potential within 2 h and remained below the hydrogen evolution potential for hours; it then increased above the hydrogen evolution potential after full charging.

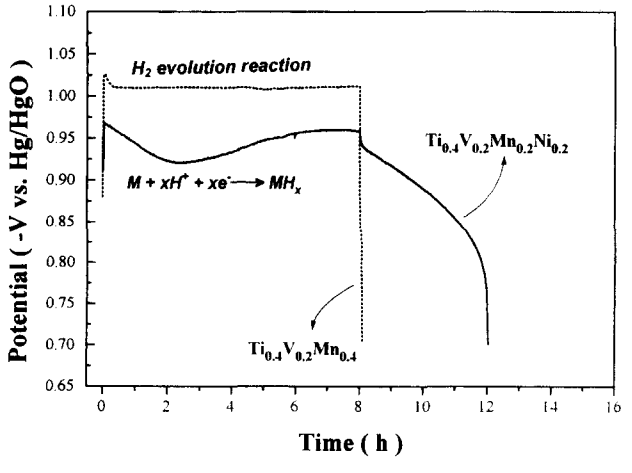

Fig. 5. Charging and discharging curves of $Ti_{0.4}V_{0.2}Mn_{0.4}$ and $Ti_{0.4}V_{0.2}Mn_{0.2}Ni_{0.2}$ at 30°C.

The $Ti_{0.4}V_{0.2}Mn_{0.2}Ni_{0.2}$ electrode was discharged for about 4 h at a current density of 50 mA g^{-1}. In contrast to the $Ti_{0.4}V_{0.2}Mn_{0.4}$ alloy, which did not contain nickel, the $Ti_{0.4}V_{0.2}Mn_{0.2}Ni_{0.2}$ alloy could be charged and discharged, and after the first cycle in KOH electrolyte showed an initial discharge capacity of 206 mA h g^{-1} at a current density of 50 mA g^{-1}. In order to investigate the electrocatalytic activity of nickel in the Ti–V–Mn–Ni alloy system, the exchange current density was evaluated by a linear polarization method. In Fig. 6, the exchange current densities are shown as a function of nickel atomic concentration in the $Ti_{0.4}V_{0.2}Mn_{0.4-x}Ni_x$ alloys. The exchange current density increased with increasing nickel concentration and that of $Ti_{0.4}V_{0.2}Mn_{0.2}Ni_{0.2}$ alloy was about ten times that of the $Ti_{0.4}V_{0.2}Mn_{0.4}$ alloy. In the Ti–V–Mn–Ni system, it was found that the electrocatalytic activity increased as the nickel concentration increased, and the $Ti_{0.4}V_{0.2}Mn_{0.2}Ni_{0.2}$ alloy was able to be hydrogenated electrochemically in KOH electrolyte because its exchange current density was much higher than that of the Ti–V–Mn alloy.

3.3. Ti–Zr–V–Mn–Ni system

In spite of the improved electrochemical hydrogenation properties of the Ti–V–Mn–Ni alloys, their gaseous hydrogenation characteristics deteriorated. The reversible hydrogen storage capacity decreased and the equilibrium desorption pressure in creased above 1 atm, as shown in Fig. 7. Accordingly, in order to increase reversible hydrogen storage capacity as

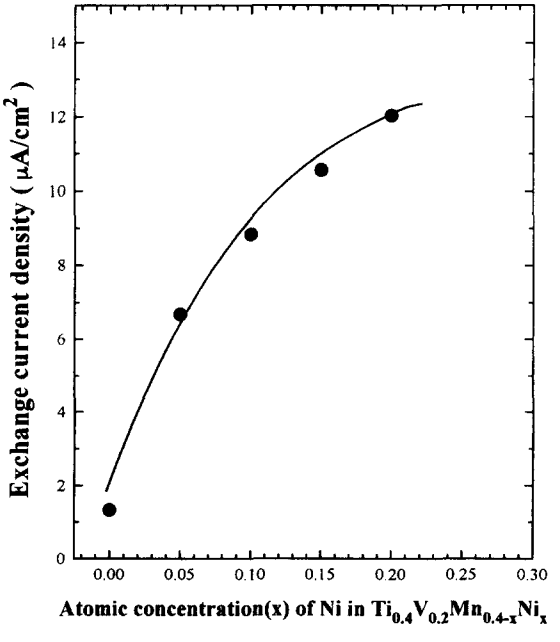

Fig. 6. Exchange current density of $Ti_{0.4}V_{0.2}Mn_{0.4-x}Ni_x$ as a function of Ni concentration.

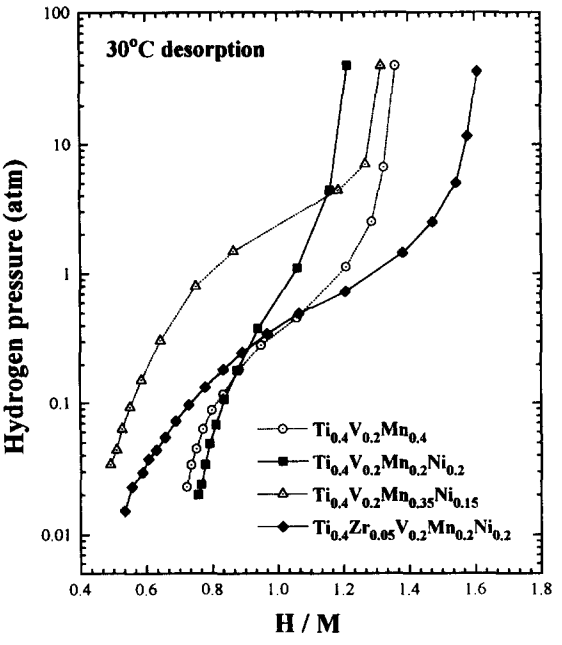

Fig. 7. Desorption *P–C* isotherms of Ti–V–Mn–Ni alloys at 30°C.

well as to adjust the equilibrium pressure to lower than 1 atm at room temperature, a small amount of zirconium was added to the Ti–V–Mn–Ni system because it has a higher affinity for hydrogen (− 188 kJ mol^{-1}) than other elements (Ti: − 137 kJ mol^{-1}, V: − 37 kJ mol^{-1}, Mn: − 25 kJ mol^{-1}). As shown in Fig. 7, the reversible hydrogen storage capacity of Ti–Zr–V–Mn–Ni alloy increased without changing the equilibrium pressure compared with Ti–V–Mn alloy. Fig. 8 shows XRD patterns of $Ti_{0.4}V_{0.2}Mn_{0.4}$, $Ti_{0.4}V_{0.2}Mn_{0.2}Ni_{0.2}$ and $Ti_{0.4}Zr_{0.05}V_{0.2}Mn_{0.2}Ni_{0.2}$ alloys.

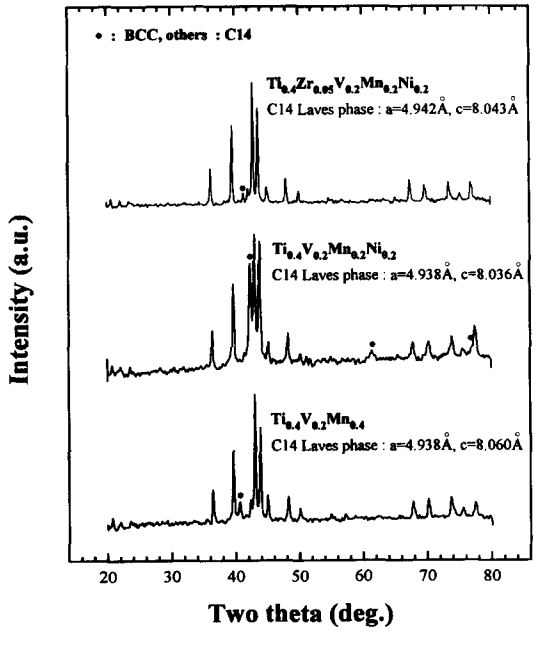

Fig. 8. XRD patterns of $Ti_{0.4}V_{0.2}Mn_{0.4-x}Ni_x$ alloys.

It was found that the peak intensity of the V-rich b.c.c. phase decreased by the addition of zirconium, whilst it increased by the addition of nickel. The unit cell volumes of the C14 Laves phase alloys remained almost the same for additions of nickel or zirconium compared with $Ti_{0.4}V_{0.2}Mn_{0.4}$ alloy. It is thought that the change of the equilibrium pressure is attributed to the change of the chemical affinity between hydrogen and alloys rather than the change of the size of the interstitial site for hydrogen; the increased reversible gaseous hydrogenation capacity of $Ti_{0.4}Zr_{0.05}V_{0.2}Mn_{0.2}Ni_{0.2}$ alloy compared with $Ti_{0.4}V_{0.2}Mn_{0.4}$ alloy is thought to be attributed to an increase in the high capacity C14 phase and a decrease in the V-rich b.c.c. phase. So, it is proposed that zirconium is suitable for the fifth element for improving hydrogenation characteristics of Ti–V–Mn–Ni alloys. Fig. 9 shows electrochemical discharge curves of the various Ti–Zr–V–Mn–Ni alloys at 30°C. In the Ti–Zr–V–Mn–Ni system, it was found that $Ti_{0.2}Zr_{0.05}V_{0.4}Mn_{0.2}Ni_{0.15}$ alloy showed the highest electrochemical discharge capacity of 440 mA h g^{-1} at a current density of 50 mA g^{-1}, and it seemed to be a promising candidate for the high capacity negative electrode material for Ni–MH battery.

In order to investigate why $Ti_{0.2}Zr_{0.05}V_{0.4}Mn_{0.2}Ni_{0.15}$ alloy has considerably higher discharge capacity, SEM, EDAX analyses and XRD measurements were carried out. From the SEM results shown in Fig. 10, it was found that $Ti_{0.2}Zr_{0.05}V_{0.4}Mn_{0.2}Ni_{0.15}$ alloy was a mixture of the matrix phase and a second phase. The composition of each phase was characterized by EDAX and both phases were prepared separately in order to investigate their structures and hydrogenation properties. It was found tnat the matrix phase was Ti-based $Ti_{0.26}Zr_{0.07}V_{0.24}Mn_{0.2}Ni_{0.23}$ alloy which had an AB_2-type C14 Laves phase structure, and the second phase was characterized as V-rich $Ti_{0.11}V_{0.66}Mn_{0.23}$ which had a b.c.c. structure. The SEM micrograph is shown in Fig. 10 and the XRD patterns are shown in Fig. 11. Fig. 12 shows desorption *P–C* isotherms of the original alloy and its C14 matrix phase and V-rich b.c.c. second phase measured at 50°C. The desorption plateau pressure of the matrix phase is in the range of 1–10 atm and that of the V-rich b.c.c. phase is 1 atm at 50°C. In the *P–C* isotherm of the b.c.c. phase there exists a low pressure plateau; this is thought to be related to the irreversible hydrogen absorption, such as the lower plateau in the vanadium–hydrogen system. The theoretical discharge capacity related to the reversible gaseous hydrogen storage capacity as follows:

$$C_{\text{theoretical}} = (96500 \times \text{wt.\% H g}^{-1}\text{ alloy})/3600 \text{ mA h g}^{-1} \quad (1)$$

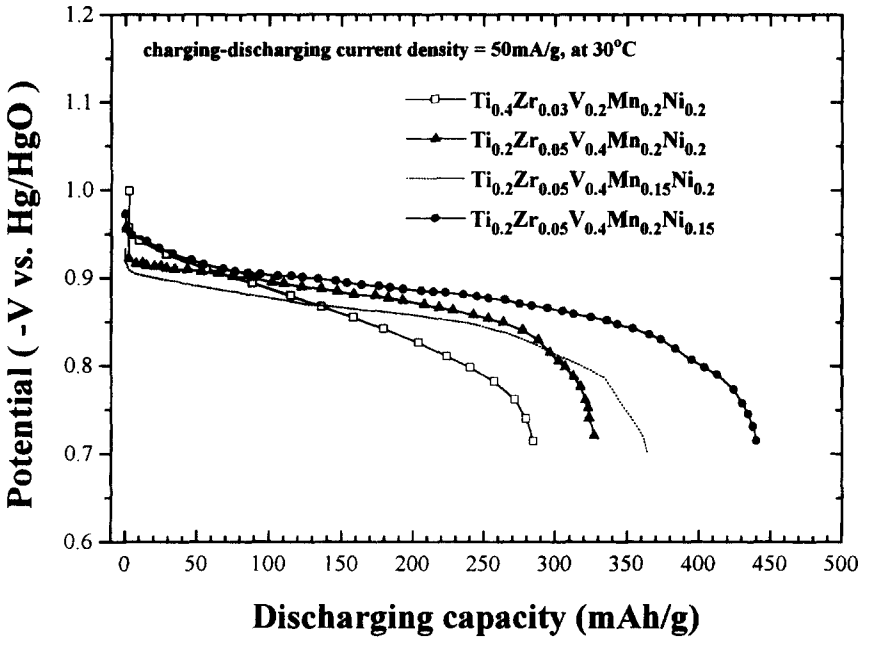

Fig. 9. Discharging curves of Ti–Zr–V–Mn–Ni alloys.

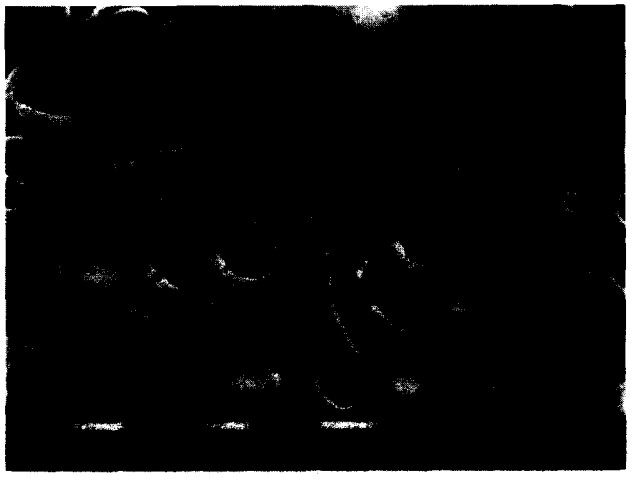

Fig. 10. Microstructure of $Ti_{0.2}Zr_{0.05}V_{0.4}Mn_{0.2}Ni_{0.15}$ alloy (white gray: matrix phase $Ti_{0.26}Zr_{0.07}V_{0.24}Mn_{0.2}Ni_{0.23}$, dark black: second phase $Ti_{0.11}V_{0.66}Mn_{0.23}$).

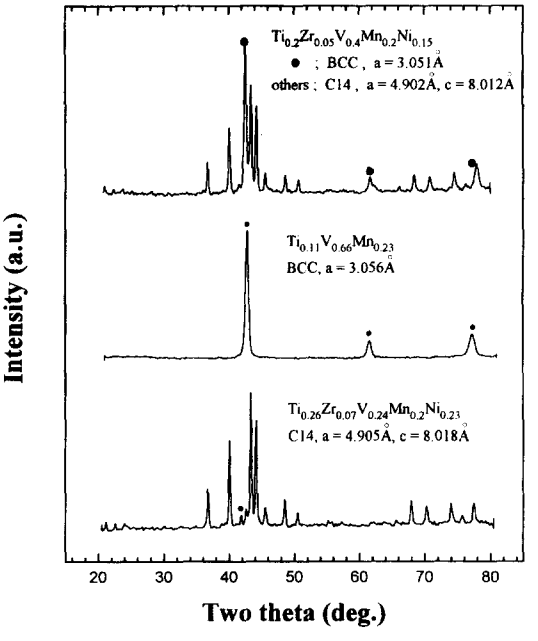

Fig. 11. XRD patterns of the $Ti_{0.2}Zr_{0.05}V_{0.4}Mn_{0.2}Ni_{0.15}$ alloy, $Ti_{0.11}V_{0.66}Mn_{0.23}$ alloy (second phase) and $Ti_{0.26}Zr_{0.07}V_{0.24}Mn_{0.2}Ni_{0.23}$ alloys (matrix phase).

The theoretical discharge capacities of the original alloy and its matrix phase alloy and second phase alloy were calculated from Eq. (1), and the values were 454 mA h g^{-1}, 386 mA h g^{-1} and 541 mA h g^{-1} respectively. The experimental electrochemical discharge capacity of the matrix phase alloy containing nickel was 360 mA h g^{-1}; however, the second phase alloy containing no nickel could not be hydrogenated in KOH electrolyte, as shown in Fig. 13. From the experimental results, it is suggested that the $Ti_{0.2}Zr_{0.05}V_{0.4}Mn_{0.2}Ni_{0.15}$ alloy composed of C14 and b.c.c. phases has a large discharge capacity because the V-rich b.c.c. phase, which has larger theoretical discharge capacity than its original alloy but cannot be electrochemically hydrogenated alone, can be hydrogenated in KOH electrolyte owing to the catalytic effect of the matrix phase which has smaller theoretical discharge capacity and contains electrocatalytic nickel as an alloying element. Even though the initial discharge capacity of this Ti-based alloy was very high, it was found that the cyclic property was poor. More work is necessary to understand the degradation

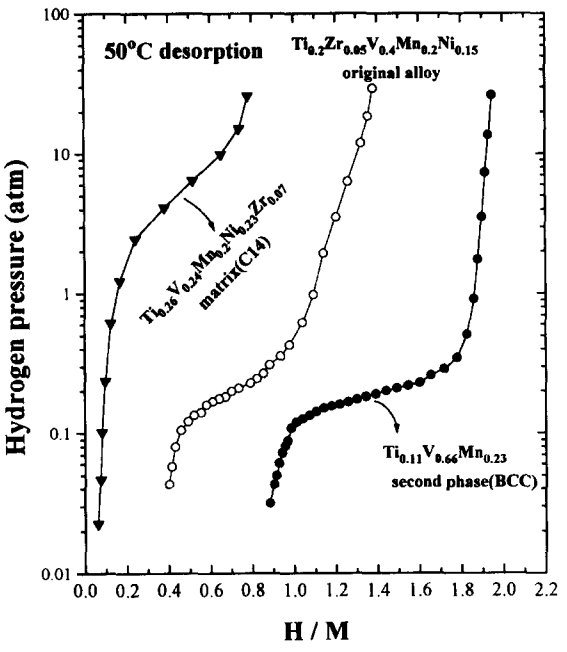

Fig. 12. Desorption P–C isotherms of the original alloy, the matrix phase alloy and the second phase alloy.

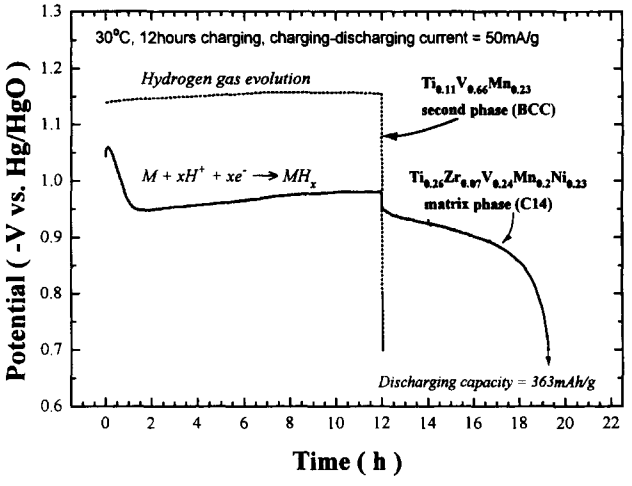

Fig. 13. Charging and discharging curves of the matrix phase and the second phase in $Ti_{0.2}Zr_{0.05}V_{0.4}Mn_{0.2}Ni_{0.15}$ alloy.

mechanism of this system in order to improve the cycle life.

4. Conclusions

The gaseous hydrogenation characteristics of Ti–Mn binary alloys were investigated by substituting V for Ti or Mn. It was found that Ni should be included in the Ti–V–Mn alloy in order to hydrogenate it electrochemically in KOH electrolyte; this is because Ni has a high catalytic activity for the charge transfer reaction in the electrochemical hydrogenation of the MH negative electrode. In confirmation, it was found that the exchange current density of the $Ti_{0.4}V_{0.2}Mn_{0.2}Ni_{0.2}$ alloy was about ten times that of the $Ti_{0.4}V_{0.2}Mn_{0.4}$ alloy. Also, zirconium was able to increase the reversible hydrogen storage capacity of Ti–V–Mn–Ni alloys, maintaining the equilibrium hydrogen desorption pressure below 1 atm at room temperature. The electrochemical discharge capacity of the Ti–Zr–V–Mn–Ni system was in the range 100–440 mA h g^{-1}; of the alloys in this system, $Ti_{0.2}Zr_{0.05}V_{0.4}Mn_{0.2}Ni_{0.15}$ showed the highest electrochemical discharge capacity of 440 mA h g^{-1}. This alloy was composed of the AB_2-type C14 Laves phase containing nickel and the V-rich b.c.c. phase which contained no nickel. The respective theoretical and experimental discharge capacities were 386 mA h g^{-1} and 360 mA h g^{-1} for the Laves phase and 541 mA h g^{-1} and 0 mA h g^{-1} for the V-rich b.c.c. phase.

It was suggested that the large discharge capacity of the $Ti_{0.2}Zr_{0.05}V_{0.4}Mn_{0.2}Ni_{0.15}$ alloy was attributed to the catalytic activity of the C14 matrix phase which utilized the large hydrogen capacity of the V-rich b.c.c. second phase. It was also found that more work is necessary to investigate the poor cyclic property of this system in order to improve the electrode properties.

References

[1] H.F. Bittner and C.C. Badcock, *J. Electrochem. Soc., 130* (1983) 193.
[2] J.J.G. Willems and K.H.J. Buschow, *J. Less-Common Met., 129* (1987) 13.
[3] M.A. Fetchenko, S. Venkatesan and S.R. Ovinsky, *Proc. Int. Symp. on Metal–Hydrogen System, Upssala, June 1992*, PII, p. 96.
[4] H. Kaiya, Advanced Ni–Cd and Ni–MH battery, *10th Int. Seminar on Primary and Secondary Battery Technology and Application, Florida, March 1–4, 1993.*
[5] S. Ovshinsky, P. Gifford, S. Venkatesan, M.A. Fetchenko, D.C. Cowigan and S. Dhar, Advancements in ovonic nickel metal hydride batteries for portable and EV applications, *10th Int. Seminar on Primary and Secondary Battery Technology and Application, Florida, March 1–4, 1993.*
[6] S. Tsuda, H. Kaiya, O. Takahashi and H. Konishi, High performance sealed small Ni–Cd and Ni–MH batteries for portable appliances, *12th Int. Seminar on Primary and Secondary Battery Technology and Application, Florida, March 6–9, 1995.*
[7] M. Oshitani, K. Takashima and Y. Matsumara, Development of a high energy density pasted nickel electrode, *Proc. Symp. on Nickel Hydroxide Electrodes, Florida, October 16–18, 1989.*
[8] M.H.J. van Rijswick, Hydrides for Energy Storage, Vol. 2, *Proc. Int. Symp., Gelio, Norway, August 14–19, 1977.*
[9] Q.M. Yang, M. Ciureanu, D.H. Ryan and J.O. Ström-Olsen, *J. Electrochem. Soc., 141* (1994) 2108.
[10] S. Wakao, Y. Yonemura, H. Nakano and H. Shimada, *J. Less-Common Met., 104* (1984) 365.
[11] S. Wakao, H. Sawa, H. Nakano, S. Chubachi and N. Abe, *J. Less-Common Met., 131* (1987) 311.
[12] S. Wakao, H. Sawa and J. Furukawa, *J. Less-Common Met., 172–174* (1991) 1219.

[13] A. Züttel, F. Meli and L. Schlapbach, *J. Alloys Compds., 203* (1994) 235.
[14] Y. Moriwaki, T. Gamo, H. Seri and T. Iwaki, *J. Less-Common Met., 172–174* (1991) 1211.
[15] S.R. Kim and J.Y. Lee, *J. Alloys Compds., 210* (1994) 109.
[16] T. Sakai, H. Yoshinaga, H. Miyamura, N. Kuriyama and H. Ishikawa, *J. Alloys Compds., 180* (1992) 37.
[17] T. Sakai, T. Hazama, N. Kuriyama, A. Kato and H. Ishikawa, *J. Less-Common Met., 172–174* (1991) 1175.
[18] M. Matsuoka, M. Terashima and C. Iwakura, *Electrochim. Acta, 38* (1993) 1087.
[19] T. Gamo, Y. Moriwaki, N. Yanagihara, T. Yamashita and T. Iwaki, *Int. J. Hydrogen Energy, 10* (1985) 39.
[20] Y. Moriwaki, T. Gamo and T. Iwaki, *J. Less-Common Met., 172–174* (1991) 1028.
[21] H. Cunmao, H. Degang and L. Qiozhu, *J. Less-Common Met., 172–174* (1991) 1044.
[22] T.B. Massalski, *Binary Alloy Phase Diagram*, American Society for Metals, Metals Park, OH, 1986.
[23] S.N. Klyamkin, V.N. Verbetsky and V.A. Demidov, *J. Alloys Compds., 205* (1994) L1.